

Inevitability and Importance of Non-Perturbative Elements in Quantum Field Theory*

Alexander P. Bakulev[†]

Bogoliubov Lab. Theor. Phys., JINR Dubna, RUSSIA

Dmitry V. Shirkov[‡]

Bogoliubov Lab. Theor. Phys., JINR Dubna, RUSSIA

ABSTRACT

The subject of the first section-lecture is concerned with the strength and the weakness of the perturbation theory (PT) approach, that is expansion in powers of a small parameter α , in Quantum Theory. We start with outlining a general troublesome feature of the main quantum theory instrument, the perturbation expansion method. The striking issue is that *perturbation series in powers of $\alpha \ll 1$ is not a convergent series*. The formal reason is an essential singularity of quantum amplitude (matrix element) $C(\alpha)$ at the origin $\alpha = 0$. In many physically important cases one needs some alternative means of theoretical analysis. In particular, this refers to perturbative Quantum Chromodynamics (pQCD) in the low-energy domain.

In the second section-lecture, we discuss the approach of Analytic Perturbation Theory (APT). We start with a short historic preamble and then discuss how combining the Dispersion Relation with the Renormalization Group (RG) techniques yields the APT with $e^{-1/\alpha}$ nonanalyticity. Next we consider the results of APT applications to low-energy QCD processes and show that in this approach the fourth-loop contributions, which appear to be on the asymptotic border in the pQCD approach, are of the order of a few per mil. Then we note that using the RG in QCD dictates the need to use the Fractional APT (FAPT) and describe its basic ingredients. As an example of the FAPT application in QCD we consider the pion form factor $F_\pi(Q^2)$ calculation. At the end, we discuss the resummation of non power series in (F)APT with application to the estimation of the Higgs-boson-decay width $\Gamma_{H \rightarrow \bar{b}b}(m_H^2)$.

* Work supported by the presidential grant Scientific School 3810.2010.2, RFBR grants No. 08-01-00686, 09-02-01149, and 11-01-00182, cooperative grant BRFB–JINR (contract No. F10D-001) and the Heisenberg–Landau Program (grant 2010–2011).

[†] E-mail address: bakulev@theor.jinr.ru

[‡] This author is responsible mainly for the text of Section 1.

1. Strength and weakness of perturbative QFT

1.1. Essential singularity at $\alpha = 0$ and functional integrals

In quantum mechanics and QFT we have a lot of successful perturbative calculations. Practically, Perturbation Theory is a synonym of Quantum Theory. Feynman diagrams became a symbol of QFT. Nevertheless, perturbative power expansion of the quantum amplitude $C(\alpha)$ is not convergent.

$$\boxed{\text{Feynman Series } \sum c_k \alpha^k \text{ is not Convergent !}}$$

The reasons for this behavior are rather simple. First, remind the Dyson argument [1]. In QED the substitution $\alpha \rightarrow -\alpha$ is equivalent¹ to $e \rightarrow ie$ and due to

$$S = T(e^{i \int L_{\text{int}}(x) dx}) = T(e^{i e \int j_\mu A^\mu dx}) \quad (1)$$

this change destroys hermiticity of Lagrangian and unitarity of S-matrix. Hence, in the complex α plane, the origin cannot be a regular point, instead, one has an essential singularity at $\alpha = 0$.

Second, in QFT one meets factorial growth of coefficients $c_k \sim k!$ and this is due to an ill-posed problem. A small parameter g standing at the highest nonlinearity is an indispensable attribute of quantum perturbation. Indeed, we quantize a linear system as a set of oscillators. Only after that we account nonlinear terms $\sim g \ll 1$ as small perturbations. However, nonlinearity usually changes the equation seriously — new solutions appear.

The most general way to analyze the issue is to use the functional integral representation. Here, for illustration purposes only, we consider the analog (often called “0-dimensional”) of the scalar field theory $g\varphi^4$

$$I(g) = \int_{-\infty}^{\infty} e^{-x^2 - gx^4} dx. \quad (2a)$$

Expanding it in power series

$$I(g) = \sum_{k=0}^{\infty} (-g)^k I_k \quad \text{with} \quad I_k = \frac{\Gamma(2k + 1/2)}{\Gamma(k + 1)} \Big|_{k \gg 1} \rightarrow 2^k k!, \quad (2b)$$

one arrives [2] at factorially growing coefficients. Meanwhile, $I(g)$ can be expressed via special MacDonal function

$$I(g) = \frac{1}{2\sqrt{g}} e^{1/8g} K_{1/4} \left(\frac{1}{8g} \right) \quad (2c)$$

with known analytic properties in the complex g plane: It is a four-sheeted function analytical in the whole complex plane besides the cut from the

¹Here $\alpha = e^2/(4\pi)$ is the QED expansion parameter, the fine structure constant.

origin $g = 0$ along the whole negative semiaxes. At the origin, it has an essential singularity $e^{-1/8g}$ and in its vicinity on the first Riemann sheet it can be written down in the Cauchy integral form:

$$I(g) = \sqrt{\pi} - \frac{g}{\sqrt{2\pi}} \int_0^\infty \frac{d\gamma e^{-1/4\gamma}}{\gamma(g + \gamma)}. \quad (2d)$$

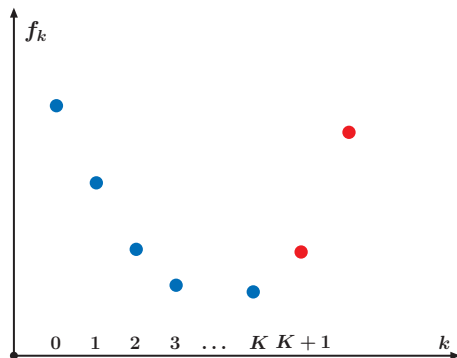
As far as the origin is not an analytical point, the power Taylor series (2b) has no convergence domain for real positive g values. This is in concert with factorial growth of power expansion coefficients. The power series is not valid also for negative g values — in accordance with Dyson's reasoning.

Besides, via 0-dimensional analog of functional integral (2a) one can illustrate the analysis of the $I(g)$ analytic properties in the complex g plane by the steepest-descent method which was devised² for the functional integral representation. Then it is possible to prove [3] factorial growth of expansion coefficients in the ϕ^4 scalar and a few other QFT models. These results have been anticipated in 1952–53 [4] just after Dyson's paper.

The same singularity structure $\sim \exp(-1/g)$ was established by improving the perturbative result using two other nonperturbative methods: Q^2 -analyticity (from Dispersion Relations), and Renormalization Invariance [5]:

$$f_{\text{pert}}(Q^2, g) = 1 - \beta_0 g \ln(Q^2) \rightarrow f_{\text{imp}}(Q^2 e^{-1/\beta_0 g}). \quad (3)$$

Henry Poincaré analysis of Asymptotic Series (AS) properties at the end of the XIX century can be summarized as follows:



The truncated AS can be used for obtaining quantitative information on expanded function. Here, the error of approximating $F(g)$ by first K terms of expansion, $F(g) \rightarrow F_K(g) = \sum_{k \leq K} f_k(g)$ is equal to the last retained term $f_K(g)$.

This yields to the existence of a *lower limit of possible accuracy* for the given g value (in contrast to convergent series!).

To elucidate the phenomenon, take a power AS, $f_k(g) = f_k g^k$ with factorial growth $f_k \sim k!$ of expansion terms $f_k(g)$ which cease to diminish at $k = K \sim 1/g$. For $k \geq K + 1$ truncation error starts to grow!

This yields the natural best possible accuracy of an AS at a given value of expansion parameter. From the explicit illustration for the function $I(g)$ (2a) with AS (2b), presented in Table 1, one can see that the optimum

²See, e.g., Section 2 in the paper[2] and references therein.

values of truncation number $K = K_* \simeq 1/(2g)$ (in dark blue) provides us with the best possible accuracy (dark blue in the last column). Indeed, an attempt to account a couple of extra terms (the second and the fourth lines) results in drastic rise of the error!

g	K	$(-g)^K I_K$	$(-g)^{K+1} I_{K+1}$	$I_K(g)$	$I(g)$	$\Delta_K I(g)$
0.07	7	-0.04(2%)	+0.07(4.4%)	1.674	1.698	1.4%
0.07	9	-0.17(10%)	+0.42(25%)	1.582	1.698	7%
0.15	2	+0.13(8%)	-0.16(10%)	1.704	1.639	4%
0.15	4	+0.30(18%)	-0.72(44%)	1.838	1.639	12%

Table 1: The last detained $((-g)^K I_K)$ and the first dismissed $((-g)^{K+1} I_{K+1})$ contributions to the power series (2b) in comparison with the exact value (2c) and the approximate result $I_K(g)$, with K being the truncation number and $\Delta_K I(g)$ — the error of approximation.

Thus, one has $K_*(g = 0.07) = 7$ and $K_*(g = 0.15) = 2$. It is not possible at all to get the 1% accuracy for $g = 0.15$.

In QED this ‘divergence menace’ is not actual, as the real expansion parameter is quite small: $\alpha/\pi \sim 1/(137\pi) \sim 2 \cdot 10^{-3}$. At the same time, in perturbative QCD (pQCD) the expansion parameter below 5–10 GeV is not very small: $\alpha_s(Q) \sim 0.2 - 0.3$. Then for an observable $A_{\text{QCD}} = \sum_k a_k (\alpha_s)^k$ with $a_k \sim k!$ and with critical order $K \sim 3 - 5$ the danger of the pQCD series explosion is actual, see below in Table 2.

Hence, a practical Non-Perturbative approach is of utmost importance. In Section 2, we concentrate on the so-called Analytic Perturbation Theory (APT), a closed scheme, devised in the late 90s[6]. It combines information from PT with two other nonperturbative methods — Analyticity and Renormalization Group (RG). Having this in mind, we outline now the RG approach. Then ideas of the Dispersion Relation method will be presented.

1.2. RG transformation

Consider transformation $R_t [\mu_i \rightarrow \mu_k, g_i \rightarrow g_k]$ as *operation* with continuous positive parameter t , acting on a *group element* $\mathcal{G}_i = \mathcal{G}(\mu_i, g_i)$, specified by 2 coordinates μ_i and g_i ³. This operation

$$R_t \cdot \mathcal{G}_i = \mathcal{G}_k \sim R_t \{ \mu_i \rightarrow \mu_k = t\mu_i, g_i \rightarrow g_k = \bar{g}(t, g_i) \} \quad (4)$$

contains dilatation of μ and functional transformation of g_μ . The R_t group structure $R_t R_\tau = R_{t\tau}$ is provided by the functional equation (FEq)

$$\bar{g}(\tau t, g) = \bar{g}(\tau, \bar{g}(t, g)) . \quad (5)$$

Indeed, if one puts $x = \tau t$, then its LHS describes $R_{\tau t}$ acting on g , $R_{\tau t} g = \bar{g}(\tau t, g)$, while the RHS one corresponds to the two-step procedure:

³For a more detailed exposition of this material kindly address to [7].

$R_\tau \otimes R_t g = R_\tau \bar{g}(t, g) = \bar{g}(\tau, \bar{g}(t, g))$. We see that a combination of the two lines results in Eq. (5), providing the group composition law $R_{\tau t} = R_\tau \otimes R_t$. Thus, the operation R_t forms a continuous Sophus Lie (1880) group of transformations.

The RG symmetry and RG transformation are close to the notion of self-similarity, well-known in Mathematical Physics since the end of the XIX century. The Self-Similarity Transformation (SST) is a simultaneous power scaling of arguments $z = \{x, t, \dots\}$ and functions $V_i(x, t, \dots)$

$$S_\lambda : \{x \rightarrow \lambda x, t \rightarrow \lambda^\alpha t\}; \quad \{V_i(z) \rightarrow V'_i(z') = \lambda^{\nu_i} V_i(z')\} \quad (6)$$

Below, we call it the *Power Self-Similarity* (PSS) transformation.

The general solution of $\bar{g}(xt, g) = \bar{g}(x, \bar{g}(t, g))$ depends on an arbitrary one-argument function see below Eq. (8). Here, we look for a partial solution, linear in the second argument $\bar{g}(x, g) = g \cdot f(x)$. The function $f(x)$ satisfies simple FEq $f(xt) = f(x) \cdot f(t)$ with general solution: $f(x) = x^\nu$ and $\bar{g}(x, t) = g \cdot x^\nu$. Thus, RG transformation is reduced to the PSS one,

$$R_t \rightarrow \{x \rightarrow x \cdot t, g \rightarrow g \cdot t^\nu\} = S_t.$$

The PSS transformation $R_t \rightarrow S_t = \{x \rightarrow x \cdot t, g \rightarrow g \cdot t^\nu\}$ is a special case of the RG one. That is, in the RG case instead of the power law t^ν , one has *arbitrary functional* dependence. Hence, one can consider the RG transformation as a *functional* generalization of the PSS one. It is natural then to treat them as transformations of functional scaling or *Functional Self-Similarity* (FSS) transformation. In short $RG \equiv FSS$.



Figure 1: The project for poster of the 2008 RG Conference in Dubna.

Here we illustrate our statements by historical analogies. One realizes that *scaling* = change of scale = *proportional change of sizes*. This notion implies that *Bogoliubov Renormalization Group* (BRG) = distorted scaling = *change of scale with continuous change of some details*. This is illustrated by Fig. 1: in both paintings one can recognize the same person, Leonard

Euler but details are different⁴.

The symmetry of the FSS group transformations can be ‘discovered’ in different fields of physics. As the illustration, we suggest a mechanical example. Imagine an elastic rod with a fixed point (point "0") bent by some external force, e.g., gravity or pressure of a moving gas or liquid, see in the left panel of Fig.2. The form of the rod can be described by the

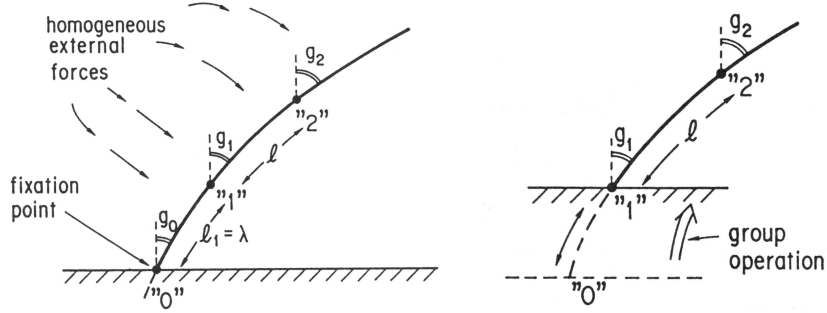


Figure 2: Elastic rod model.

angle g between tangent to the rod and vertical directions considered as a function of the distance l along the rod from the fixation point — by the function $g(l)$. If the properties of the rod material and exterior forces are homogeneous along its length (independent of l), then $g(l)$ can be expressed as function $G(l, g_0)$, depending also on g_0 — deviation angle at the fixation point from which distance l is measured. G can depend on other arguments, like extra forces and rod material parameters, but in this context they are irrelevant.

Take two arbitrary points on the rod, "1" and "2" with $l_1 = \lambda$ and $l_2 = \lambda + l$. The angles g_i at points "0", "1" and "2" are related via G function:

$$g_1 = G(\lambda, g_0), \quad g_2 = G(\lambda + l, g_0) = G(l, g_1).$$

To get the RHS of the second equation, one has to imagine that the fixation point now is "1", as shown in the right panel of Fig.2. Combining both the equations, $g_1 = G(\lambda, g_0)$ and $g_2 = G(\lambda + l, g_0) = G(l, g_1)$, one gets the group composition law $G\{\lambda, G(l, g)\} = G(\lambda + l, g)$ equivalent [via relation $\bar{g}(x, g) \equiv G(l = \ln x, g)$] to FEq for invariant coupling

$$\bar{g}(x, g) = \bar{g}\left(\frac{x}{t}, \bar{g}(t, g)\right). \quad (7a)$$

⁴The original (smaller in Fig.1) portrait was painted by E. Handmann in 1756 and is stored at Basel University, whereas the larger and more official one was painted by I. König at the request of the Russian Academy of Sciences (due to its 150-year anniversary) in 1875 as a copy from the original portrait. This newer portrait was lost during Russian revolution and discovered in a curiosity shop in 1972 by Georgy Sergeevich Golitsyn [8].

first devised in [9]. It can be represented in two infinitesimal forms: The nonlinear differential equation (DEq)

$$x \frac{\partial \bar{g}(x, g)}{\partial x} = \beta(\bar{g}(x, g)), \quad \text{with} \quad \beta(g) = t \left. \frac{\partial \bar{g}(t, g)}{\partial t} \right|_{t=1}, \quad (7b)$$

and the linear partial one (PDEq)

$$\left[x \frac{\partial}{\partial x} - \beta(g) \frac{\partial}{\partial g} \right] \bar{g}(x, g) = 0. \quad (7c)$$

In the QFT jargon, the beta-function $\beta(g)$ is known as the RG generator. Note that each of the two DEqs is equivalent to the functional one (7a) provided the normalization condition

$$\bar{g}(1, g) = g \quad (7d)$$

is satisfied. The general solution of the last FEq can be found from the relation

$$\Phi(\bar{g}) - \Phi(g) \equiv \int_g^{\bar{g}} \frac{d\gamma}{\beta(\gamma)} = \ln x. \quad (8)$$

1.3. RG effective coupling in QFT

To illustrate the power of RG-invariance, on the one hand, and the effectiveness of its differential formulation, consider now an illuminating example of the effective coupling \bar{g} UV asymptotics. In the common perturbation theory (PT), one has

$$\bar{g}_{\text{PT}}^{[1]}(x; g) = g + g^2 \beta_0 \ln x, \quad (9a)$$

— the so called one-loop UV logarithm. Here, as well as in Eqs. (7a)–(7c),

$$x = Q^2/\mu^2; \quad g = g_\mu = \bar{g}(x; g); \quad Q^2 = \mathbf{Q}^2 - Q_0^2 > 0.$$

Evidently, expression (9a) is not RG-invariant. Indeed, substituting it into the functional equation (5) one obtains the discrepancy

$$\begin{aligned} \Delta_{\text{discr}} \left[\bar{g}_{\text{PT}}^{[1]} \right] &\equiv \bar{g}_{\text{PT}}^{[1]}(x; g) - \bar{g}_{\text{PT}}^{[1]} \left(\frac{x}{t}, \bar{g}_{\text{PT}}^{[1]}(t; g) \right) \\ &= [g + g^2 \beta_0 \ln x] - [g + g^2 \beta_0 \ln x + 2g^3 \beta_0^2 \ln t \ln(x/t)] \neq 0 \end{aligned}$$

— error of the g^3 -order that can be killed by adding to starting approximation (9a) the next-order term $g^3 \beta_0^2 \ln^2 x$ etc. The final result of this iterative restoring is the famous sum of geometric progression

$$\bar{g}_{\text{RG}}^{[1]}(x; g) = g \sum_{k \geq 0} (g \beta_0 \ln x)^k = \frac{g}{1 - g \beta_0 \ln x} \quad (9b)$$

which sums up the leading order (LO) logarithms $g(g \ln x)^k$. On the other hand, this solution can be immediately obtained by analytical means via the first differential RG Eq.(7b) with $\beta(g) = \beta_0 g^2$, obtained from Eq. (9a). Starting with the two-loop perturbative UV asymptotics

$$\bar{g}_{\text{PT}}^{[2]}(x; g) = g + g^2 \beta_0 \ln x + g^3 (\beta_0^2 (\ln x)^2 + \beta_1 \ln x) \quad (10a)$$

one gets (again in few lines of calculations by RG technique) the Next-to-Leading-Order (NLO) approximate (at $\ln x \gg 1$) result

$$\bar{g}_{\text{RG}}^{[2]}(x; g) \simeq \frac{g}{1 - g \beta_0 \ln x - g^2 \beta_1 \ln(\ln x)}. \quad (10b)$$

Illustration in QED. In QED, due to gauge invariance (Ward identities), the RG-invariant coupling reduces (see, pioneer review paper [9] and references therein as well as Sect. 48.1 in monograph [10]) to the transverse amplitude of the dressed photon propagator

$$\bar{\alpha}(Q^2, \alpha) = \alpha d_{tr}(Q^2, \alpha). \quad (11)$$

Originally, it was introduced there as a function describing the RG transformation of a PT expansion parameter. In a proper QED (quantum electrodynamics of electrons, positrons and photons) its one-loop expression reads

$$\bar{\alpha}_{\text{PT}}^{[1]}(x; \alpha_\mu) = \alpha_\mu + \frac{\alpha_\mu^2}{3\pi} \ln x; \quad x = \ln(Q^2/\mu^2). \quad (12)$$

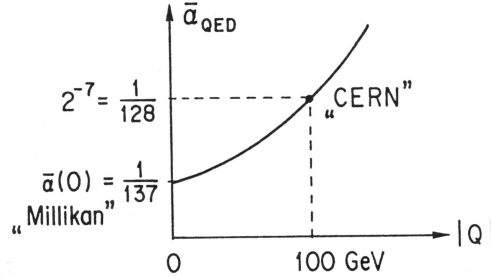


Figure 3: Artistic view on experimental verification of the $\bar{\alpha}_{\text{QED}}$ “running” (solid line).

In a sense, it is a generalization of the electron effective charge⁵ introduced first by Dirac [11]:

$$e(Q) \simeq e \left[1 + \frac{e^2}{12\pi^2} \ln \left(\frac{Q}{m_e} \right) + \dots \right]. \quad (13a)$$

⁵Its Fourier image is the charge $Q(r)$ of point electron screened by quantum vacuum fluctuations.

After the RG machinery, (12) takes the invariant form

$$\bar{\alpha}_{\text{QED}}(Q^2) \simeq \frac{\alpha_\mu}{1 - (\alpha_\mu/(3\pi)) \ln(Q^2/\mu^2)}. \quad (13b)$$

Its contemporary Standard Model analog was checked experimentally about a decade ago at LEP, the e^+e^- -collider at CERN, see results in Fig. 3.

Note also that the Bogoliubov RG was initially devised in a mass-dependent form [9]. Starting, e.g., with the mass-dependent one-loop PT

$$\bar{g}_{\text{PT}}^{[1]}(x, y; g) = g + g^2 [I_1(x/y) - I_1(1/y)] \quad (14a)$$

with $x = q^2/\mu^2$ and $y = m^2/\mu^2$, one gets

$$\bar{g}_{\text{RG}}^{[1]}(x, y; g) = \frac{g}{1 - g [I_1(x/y) - I_1(1/y)]} \quad (14b)$$

and, similarly at the two-loop level[12]. This *massive* RG provides us with means to make an accurate matching across the heavy-quark thresholds, both in QCD and in Grand Unification.

1.4. Analyticity from causality in QFT

Turn now to the *Dispersion Relation Method* that relates causality in space-time with analyticity in kinematic (energy, momentum transfer) variables.

To illustrate the main idea, consider the Fourier image

$$F(E) = \int_{-\infty}^{\infty} e^{itE} A(t) dt \quad (15)$$

of the forward scattering amplitude $A(t)$, being subdued to the nonrelativistic *causality condition*:

$$A(t) = 0 \quad \text{at} \quad t < 0. \quad (16)$$

In this case, $F(E)$ can be analytically continued from real E values to the upper half of the complex plane $Q \rightarrow z = E + i\xi$; $\xi = \text{Im} z > 0$, since the factor $e^{-t\xi}$ in the integrand provides convergence of the integral for $F(z)$. Using then the Cauchy theorem with integration contour Γ^+ in the upper half-plane and z inside Γ^+

$$F(z) = \frac{1}{2\pi i} \oint_{\Gamma^+} \frac{F(z')}{z' - z} dz'$$

one can get *Dispersion Relation* for the forward scattering amplitude

$$\text{Re} F(E) = \frac{1}{\pi} \mathcal{P} \int_{-\infty}^{\infty} \frac{\text{Im} F(E')}{E' - E} dE' = \mathcal{P} \int_m^{\infty} \frac{k\sigma(E')}{E' - E} dE', \quad (17)$$

relating two observable functions. In obtaining this non-subtracted dispersion relation we tacitly assumed “good” $F(z)$ asymptotic behavior and used *Optical Theorem* $\mathbf{Im}F(E) = k \sigma(E)$. In a more realistic case, one starts with relativistic causality and adds symmetry crossing property of the forward scattering amplitude.

Remind that instead of the Pauli–Jordan commutator

$$D(x - y) = \frac{1}{i} \langle 0 | [\phi(x), \phi(y)] | 0 \rangle, \quad (18a)$$

(vanishing outside the light cone at $(x - y)^2 = (x_0 - y_0)^2 - (\mathbf{x} - \mathbf{y})^2 < 0$ and involved in relativistic-invariant quantization) in construction of matrix elements and observables one needs the Stueckelberg–Feynman causal propagator

$$D_c(x - y) = D_F(x - y) = \frac{1}{i} \langle 0 | T [\phi(x) \phi(y)] | 0 \rangle, \quad (18b)$$

being the vacuum expectation value of the time-ordered product. Just this function (and its derivatives) enters into Feynman rules.

At the same time, in the Schwinger–Dyson equations one deals with its “dressed” version which includes radiative corrections

$$D_{\text{dress}}(x; g) = \frac{1}{i S_0} \langle 0 | T [\phi(x) \phi(0) S(g)] | 0 \rangle, \quad (18c)$$

from the scattering matrix

$$S(g) = 1 + g S_1 + g^2 S_2 + \dots$$

This dressed causal propagator can be represented in the Källén–Lehmann spectral form⁶

$$D_{\text{dress}}(q^2, g) = \frac{1}{m^2 - q^2 - i\varepsilon} + \frac{1}{\pi} \int_{m_1}^{\infty} \frac{\rho(\sigma, g) d\sigma}{\sigma - q^2 - i\varepsilon} \quad (18d)$$

This representation, in a sense, resembles the forward dispersion relation (17). Here, quite similarly, it defines the function $D(z) \equiv D_{\text{dress}}(z, g)$ analytic in the whole complex plane z except the pole and the cut on part of the real axis. In its proof, as well, the relativistic generalization of the causality condition (16) is used.

In what follows, we have to combine two nonperturbative methods — the RG and the Dispersion Relation ones.

⁶Here we give its simplest, nonsubtracted version that is valid for the appropriately decreasing spectral density behaving as $\rho(\sigma, g) \lesssim 1/\ln^2 \sigma$.

1.5. RG and causality

Return to the QED invariant coupling. According to Eq. (11), it is proportional to the transverse amplitude of the dressed photon propagator. As it was first shown by Källén [13], the latter amplitude can be represented in the form congeneric to Eq. (18d). Hence, the same presentation

$$\bar{\alpha}(Q^2, \alpha) = \frac{1}{\pi} \int_0^{\infty} \frac{\rho(\sigma, \alpha) d\sigma}{\sigma + Q^2 - i\epsilon} \quad (19)$$

has to be valid for the QED effective coupling. That is, the function $\bar{\alpha}(z, \alpha)$ should be analytic in the duly cut complex z plane. This is true, term-by-term, for its PT expansion, like Eq. (12). However, it is not true for its RG-invariant counterpart, Eq. (13b), as it contains parasitic singularity outside the allowed cut — the so-called ghost or Landau pole at

$$Q^2 = Q_*^2 = \mu^2 e^{3\pi/\alpha_\mu}. \quad (20)$$

An elegant solution to resolve the issue was proposed by Bogoliubov et al. [14]. Omitting the details we mention here the main recipe:

To bring a RG-invariant but singular (containing extra pole) expression in the proper Q^2 -analytic form, one has to use the spectral representation (19) with the spectral density ρ defined from the related PT input, Eq. (13b).

The resulting *analyticized* expression is

$$\bar{\alpha}_{\text{an}}(x, \alpha_\mu) = \frac{\alpha_\mu}{1 - \alpha_\mu/(3\pi) \ln x} + \frac{3\pi}{x - x_*}; \quad x_* \equiv e^{3\pi/\alpha_\mu}. \quad (21)$$

The second term in the RHS is invisible in the PT expansion. Remarkably, it contains an essential singularity at $\alpha = 0$ of a proper type.

1.6. QCD effective coupling

In QCD, at the one-loop, LO approximation one has

$$\alpha_s^{(1)}(Q) = \frac{\alpha_s(\mu)}{1 + \alpha_s(\mu)\beta_0 \ln(Q^2/\mu^2)} = \frac{1}{\beta_0 L_Q}, \quad L_Q = \ln\left(\frac{Q^2}{\Lambda^2}\right). \quad (22)$$

The NLO, or two-loop expression in the Denominator Representation contains log-of-log dependence (just like in eq.(10b) for $L_Q \gg 1$):

$$\alpha_s^{(2)}(Q) \simeq \frac{1}{\beta_0 L_Q + (\beta_1/\beta_0) \ln L_Q}; \quad \beta_{0,1} \sim 1. \quad (23)$$

Note that the famous Asymptotic Freedom UV behavior $\alpha_s(Q) \sim 1/L_Q$ is correct already in the LO approximation. The QCD scale Λ turns out to

be numerically close to the confinement scale $\Lambda \sim 300 - 400 \text{ MeV} \simeq 2 m_\pi$; that is $R_\Lambda \sim 10^{-13} \text{ cm}$.

The QCD final product is formulae for hadronic observables. Some of them, e. g., the ratio of inclusive cross-sections for e^+e^- annihilation, can be directly expressed

$$R_{e^+e^-}(s) = \frac{\sigma_{e^+e^- \rightarrow \text{hadrons}}(s)}{\sigma_{e^+e^- \rightarrow \mu^+\mu^-}(s)} = R(s; \alpha_s) \quad (24a)$$

in terms of the QCD notions. As an RG-invariant this ratio *should depend on the QCD coupling $\alpha_s(s)$ only!* Perturbatively, it is power functional expansion

$$R(s; \alpha_s) = R_{\text{inv}}(\alpha_s(s)) = 1 + r_1 \alpha_s(s) + r_2 \alpha_s^2(s) + O(\alpha_s^3(s)) . \quad (24b)$$

Remarkably that, according to the 2007 Bethke review [15], above a few GeV the two-loop pQCD nicely correlates all $\alpha_s(Q^2)$ data, see Fig. 4.

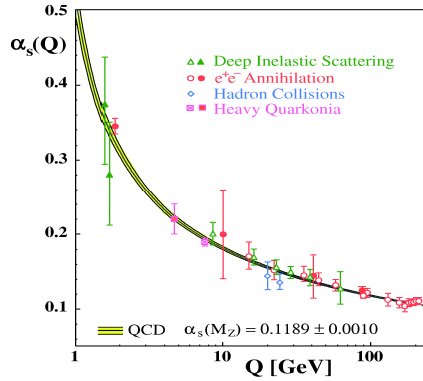


Figure 4: Triumph of the NLO pQCD from 200 up to 3 – 5 GeV (taken from [15]).

However, data below 5 GeV are not good enough: One can see from Table 2 that while the situation with higher-loop corrections for the $R_{e^+e^-}$ ratio is rather good (the first line), the Bjorken Sum Rule (SR) case (the third line) delivers to us a signal of possible blow-up (like in Table 1) of the related

Observable	Scale	1-loop	2-loop	3-loop	4-loop	Δ_{exp}
$R_{e^+e^- \rightarrow \text{hadrons}}$	10 GeV	92%	7.6%	1.0%	-0.6%	12–30%
R_τ in τ -decay	2 GeV	51%	27%	14%	8%	5%
Bjorken SR	2 GeV	56%	21%	12%	11%	6%

Table 2: Relative size of 1-, 2-, 3-, and 4-loop contributions to observables. Two last lines are taken from [16]. Three-loop estimations can be found in [17].

asymptotic perturbative series at $Q \lesssim 2 - 3$ GeV. Just in this region the PDG canonized explicit expression for $\alpha_s(Q^2)$ starts to grow sharply as even the one-loop expression for effective QCD coupling

$$\alpha_s^{(1)}(Q) = \frac{1}{\beta_0 \ln(Q^2/\Lambda^2)} \sim \frac{1}{\beta_0 (Q^2 - \Lambda^2)} \quad \text{at } Q^2 \sim \Lambda^2 \quad (25)$$

has *unphysical* (Landau) singularity. Just this singularity at $|Q| = \Lambda \sim 350$ MeV prevents from analyzing data by pQCD in the low-energy physical region below few GeV.

Meanwhile, all nonperturbative lattice-QCD simulations testify to regularity of $\alpha_s(Q)$ behavior in the $Q^2 \sim \Lambda^2$ region — see fresh overviews [18]. In what follows, we shall deal with ghost-free analytic QCD couplings (and their powers) taken from the APT and its generalization which are regular in the low-energy region and in the high-energy one coincide with the common $\alpha_s(Q^2)$.

2. Analytic Perturbative Theory (APT) in QCD

2.1. APT: Historic Preamble

As it has been mentioned above in Sect. 1.5., the analytization recipe is a common product of two nonperturbative methods — the RG and DR ones. Originally, it was formulated [14] for QED in the Euclidean region. Then in 1982 Radyushkin and Krasnikov&Pivovarov [19] using the dispersion technique suggested regular (for $s \geq \Lambda^2$) QCD running couplings in the Minkowski region, namely $\pi^{-1} \arctan(\pi/L_s)$ and $\Phi(\alpha_s^n[L_s])$, $L_s = \ln(s/\Lambda^2)$, with indication of the need to use the non power expansion in $\Phi(\alpha_s^n[L_s])$ instead of the power one. The real proliferation of this technique into QCD was initiated by Igor Solovtsov and his co-authors in the mid-90s [6]. In these pioneer papers, the ghost-free expressions for the RG-invariant QCD couplings in both the energy-like Minkowskian region and the momentum-transfer Euclidean one were obtained. Quite soon this construction was developed [20] in a closed scheme.⁷ See the history details in the recent review paper [17]. The whole construction is known since then as the Analytic Perturbation Theory.⁸

The next step, made by Bakulev, Mikhailov, and Stefanis, generalizes the APT by including fractional powers of coupling, as well as products of coupling powers and logarithms [23] and for this reason, it was named the *Fractional APT*. At the same time, it appears possible to sum up non power series in the (F)APT [24, 25].

⁷The essential point was discovering the necessity of non power type of functional expansions [21] which are the only compatible ones with linear integral transformations relating Euclidean, Minkowski and space position pictures.

⁸Close results were partly obtained by Simonov using the background perturbation theory [22].

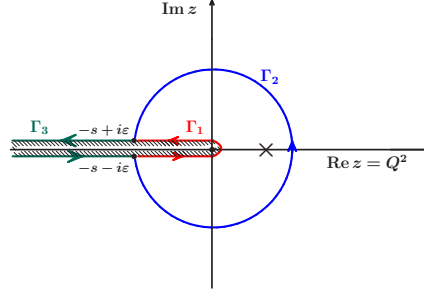


Figure 5: Contours of integration on the road to the Minkowski space.

2.2. Basics of APT

In the standard pQCD, as we described in Sect. 1, the one-loop RG equation for the effective coupling $\alpha_s(Q^2) = a[L]/\beta_f$ with $L = \ln(Q^2/\Lambda^2)$ and $\beta_f = \beta_0(N_f) = (11 - 2N_f/3)/(4\pi)$ generates the pole singularity, $a[L] = 1/L$.

Due to this pole, in pQCD the problem arises: How to go to the Minkowski region? Quantities in the Minkowski region are usually represented by contour integrals of the type $\oint f(z)D(z)dz$. In the integrands one uses $D(z) = \sum_m d_m \alpha_s^m(z)$ and changes the integration contour to Γ_i . This change of the integration contour is legitimate if $D(z)f(z)$ is analytic inside the circle everywhere. But $\alpha_s(z)$ and hence $D(z)f(z)$ have the Landau pole singularity just inside! In the APT effective couplings $\mathcal{A}_n(z)$ are analytic functions and this problem does not appear at all! In [25] (2010) the equivalence of the Contour-Improved-PT (CIPT) approach to the (F)APT for quantities like $R(s)$ was proved, which can be symbolically expressed as

$$\boxed{\text{CIPT} \left\{ \oint_{\Gamma_2} \frac{D(z)dz}{z} \right\} = \text{(F)APT} \left\{ \oint_{\Gamma_3} \frac{D(z)dz}{z} \right\}.}$$

By the analytization in the APT for an observable $f(Q^2)$ we mean the Källén–Lehmann representation (18d)

$$[f(Q^2)]_{\text{an}} = \int_0^\infty \frac{\rho_f(\sigma)}{\sigma + Q^2 - i\epsilon} d\sigma \quad (26)$$

with $\rho_f(\sigma) = \frac{1}{\pi} \text{Im} [f(-\sigma)]$. Then in the one-loop approximation $\bar{\rho}_1(\sigma) =$

$1/\sqrt{L_\sigma^2 + \pi^2}$ and⁹

$$\bar{\mathcal{A}}_1[L] = \int_0^\infty \frac{\bar{\rho}_1(\sigma)}{\sigma + Q^2} d\sigma = \frac{1}{L} - \frac{1}{e^L - 1}, \quad (27a)$$

$$\bar{\mathfrak{A}}_1[L_s] = \int_s^\infty \frac{\bar{\rho}_1(\sigma)}{\sigma} d\sigma = \frac{1}{\pi} \arccos \frac{L_s}{\sqrt{\pi^2 + L_s^2}}, \quad (27b)$$

whereas analytic images of the higher powers ($n \geq 2, n \in \mathbb{N}$) are:

$$\begin{pmatrix} \bar{\mathcal{A}}_n[L] \\ \bar{\mathfrak{A}}_n[L_s] \end{pmatrix} = \frac{1}{(n-1)!} \left[-\frac{d}{dL} \right]^{n-1} \begin{pmatrix} \bar{\mathcal{A}}_1[L] \\ \bar{\mathfrak{A}}_1[L_s] \end{pmatrix}. \quad (27c)$$

Note that at $L \gg 1$ the pole remover $\sim e^{-L} \approx e^{-1/a}$. In other words, Källén–Lehmann analyticity in the Q^2 plane generates nonperturbative e^{-1/α_s} correction. This correction guarantees the absence of spurious Landau-pole singularity and ensures the correspondence with PT $\alpha_s(Q^2)$ at $Q^2 \gg 1 \text{ GeV}^2$.

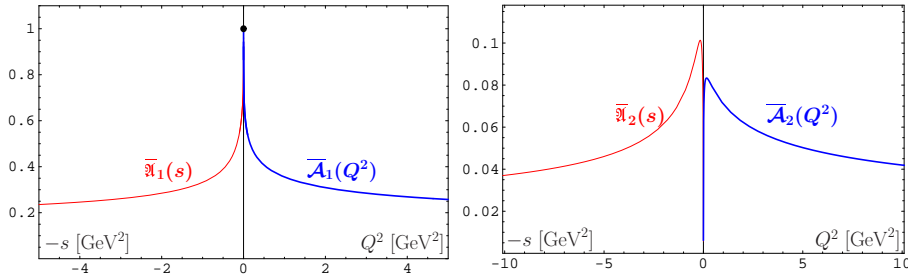


Figure 6: Distorting Mirror for analytic couplings in the Minkowski and Euclidean regions. Left panel: for $\bar{\mathfrak{A}}_1(s)$ and $\bar{\mathcal{A}}_1(Q^2)$. Right panel: for $\bar{\mathfrak{A}}_2(s)$ and $\bar{\mathcal{A}}_2(Q^2)$.

In Fig. 6, we show the so-called Distorting Mirror for analytic couplings in the Minkowski and Euclidean regions: in the left panel — for $\bar{\mathfrak{A}}_1(s)$ and $\bar{\mathcal{A}}_1(Q^2)$, whereas in the right panel — for $\bar{\mathfrak{A}}_2(s)$ and $\bar{\mathcal{A}}_2(Q^2)$. We see that in the IR domain one has universal finite IR values $\bar{\mathcal{A}}_1(0) = \bar{\mathfrak{A}}_1(0) = 1$. Moreover, starting from the two-loop level analytic couplings reveal loop stabilization of IR behavior. This yields practical loop- and renormalization-scheme-independence of $\mathcal{A}_1(Q^2)$, $\mathfrak{A}_1(s)$, and higher expansion functions, for details see [17].

⁹We use the notation $f(Q^2)$ and $f[L]$ in order to specify the arguments we mean — squared momentum Q^2 or its logarithm $L = \ln(Q^2/\Lambda^2)$, that is $f[L] = f(\Lambda^2 \cdot e^L)$ and Λ^2 is usually referred to the $N_f = 3$ region. Note that here we introduced the notation $\bar{\mathcal{A}}_n[L]$ and $\bar{\mathfrak{A}}_n[L]$ in order to distinguish analytic images of normalized coupling powers, $a^n(Q^2)$, from the corresponding images of $\alpha_s^n(Q^2)$ — for the letters we use the standard notation $\mathcal{A}_n[L]$ and $\mathfrak{A}_n[L]$. This notation is different from that used in [23, 25].

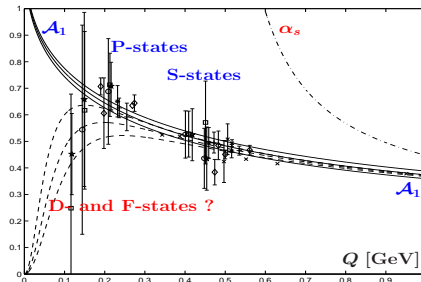


Figure 7: Comparing α_s^{exp} from the meson spectrum and the three-loop \mathcal{A}_1 at $\Lambda_{n_f=3}^{(3)} = (417 \pm 42) \text{ MeV}$ (solid lines). The three-loop α_s is shown as the dot-dashed line.

In Fig. 7, we show the results of the APT application in meson spectroscopy obtained in [26]. We observe from this comparison that the three-loop α_s , shown as dot-dashed line, is completely excluded, whereas the three-loop APT coupling goes through all the “experimental” points due to well-established P - and S -wave meson states.

In the APT, in addition to the regular behavior of couplings, one has to have non power expansions for physical observables. Indeed, if in the standard pQCD for an observable D we have¹⁰

$$\mathcal{D}_{\text{PT}}(Q^2) = d_0 + d_1 \alpha_s(Q^2) + d_2 \alpha_s^2(Q^2) + d_3 \alpha_s^3(Q^2) + \dots; \quad (28a)$$

$$\mathcal{R}_{\text{PT}}(s) = d_0 + d_1 \alpha_s(s) + d_2 \alpha_s^2(s) + r_3 \alpha_s^3(s) + \dots, \quad (28b)$$

then in the APT we should use the non power functional expansion

$$\mathcal{D}_{\text{APT}}(Q^2) = d_0 + d_1 \mathcal{A}_1(Q^2) + d_2 \mathcal{A}_2(Q^2) + d_3 \mathcal{A}_3(Q^2) + \dots; \quad (28c)$$

$$\mathcal{R}_{\text{APT}}(s) = d_0 + d_1 \mathfrak{A}_1(s) + d_2 \mathfrak{A}_2(s) + d_3 \mathfrak{A}_3(s) + \dots. \quad (28d)$$

This provides

- Better loop convergence (compare Tables 2 and 3) and practical renormalization-scheme independence of observables;
- Third terms in (28c) and (28d) contribute less than 5%, cf. Table 3. Again the two-loop ($N^2\text{LO}$) level is sufficient.

2.3. From APT to FAPT

At first glance, the APT is a complete theory providing tools to produce an analytic answer for any perturbative series in QCD. However, in 2001 Karanikas and Stefanis [28] suggested the principle of analytization “as a whole” in the Q^2 plane for hadronic observables, calculated perturbatively. More precisely, they proposed the analytization recipe for terms like

¹⁰Here r_3 and higher-order coefficients r_n differ from d_3 and d_n by the π^2 terms.

Observable	Scale	1-loop	2-loop	3-loop	4-loop	Δ_{exp}
$R_{e^+e^- \rightarrow \text{hadrons}}$	10 GeV	92.2%	7%	0.7%	0.1%	12–30%
R_τ in τ -decay	2 GeV	90.6%	8.2%	1%	0.2%	5%
Bjorken SR	2 GeV	75%	20.5%	4.55%	−0.05%	6%

Table 3: Relative size of 1-, 2-, 3-, and 4-loop contributions to observables in the APT (for comparison with PT — see Table 2 in Section 1.6.). Estimates on R_τ are taken from [27], whereas those on Bjorken SR — from the paper in preparation [16] (the 3-loop estimations can be found in [17]).

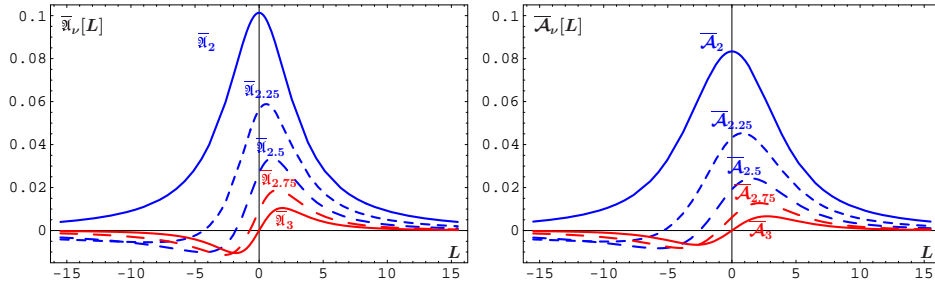


Figure 8: Comparing $\bar{\mathfrak{A}}_\nu[L]$ (left panel) and $\bar{\mathcal{A}}_\nu[L]$ (right panel) vs. L for fractional $\nu \in [2, 3]$.

$\int_0^1 dx \int_0^1 dy \alpha_s(Q^2 xy) f(x) f(y)$ which can be treated as an effective account for the logarithmic terms in the next-to-leading-order approximation of the pQCD. Indeed, in the standard pQCD one also has:

(i) the factorization procedure in QCD that gives rise to the appearance of logarithmic factors of the type: $a^\nu[L] L$;

(ii) the RG evolution that generates evolution factors of the type:

$B(Q^2) = [Z(Q^2)/Z(\mu^2)] B(\mu^2)$ which reduce in the one-loop approximation to $Z(Q^2) \sim a^\nu[L]$ with $\nu = \gamma_0/(2\beta_0)$ being a fractional number.

All that means that in order to generalize the APT in the “analytization as a whole” direction, one needs to construct analytic images of new functions: a^ν , $a^\nu L^m$, \dots . This task was performed in the framework of the so-called FAPT suggested in [23]. Now we briefly describe this approach.

In the one-loop approximation, using recursive relation (27c) we can obtain explicit expressions for $\bar{\mathcal{A}}_\nu[L]$ and $\bar{\mathfrak{A}}_\nu[L]$:

$$\bar{\mathcal{A}}_\nu[L] = \frac{1}{L^\nu} - \frac{F(e^{-L}, 1 - \nu)}{\Gamma(\nu)}; \quad (29a)$$

$$\bar{\mathfrak{A}}_\nu[L] = \frac{\sin \left[(\nu - 1) \arccos \left(L / \sqrt{\pi^2 + L^2} \right) \right]}{\pi(\nu - 1) (\pi^2 + L^2)^{(\nu-1)/2}}. \quad (29b)$$

Here $F(z, \nu)$ is the reduced Lerch transcendental function which is an analytic function in ν . The couplings $\overline{\mathcal{A}}_\nu[L]$ and $\overline{\mathfrak{A}}_\nu[L]$ have very interesting properties, which we discussed extensively in our previous papers [23].

In Fig. 8, we show in comparison how $\overline{\mathfrak{A}}_\nu[L]$ and $\overline{\mathcal{A}}_\nu[L]$ depend on L for fractional values of ν : one more time we observe the same picture of the Distorting Mirror when comparing the Minkowski (left panel) and Euclidean (right panel) regions.

To demonstrate the importance of taking into account the FAPT, that is using $\mathcal{A}_\nu[L]$ and $\mathfrak{A}_\nu[L]$ instead of $(\mathcal{A}_1[L])^\nu$ and $(\mathfrak{A}_1[L])^\nu$, we show in Fig. 9 the values of the normalized deviations $\Delta_M(L, \nu) = 1 - (\mathfrak{A}_1[L])^\nu / \mathfrak{A}_\nu[L]$ and $\Delta_E(L, \nu) = 1 - (\mathcal{A}_1[L])^\nu / \mathcal{A}_\nu[L]$ in the Minkowski and Euclidean domains, respectively.

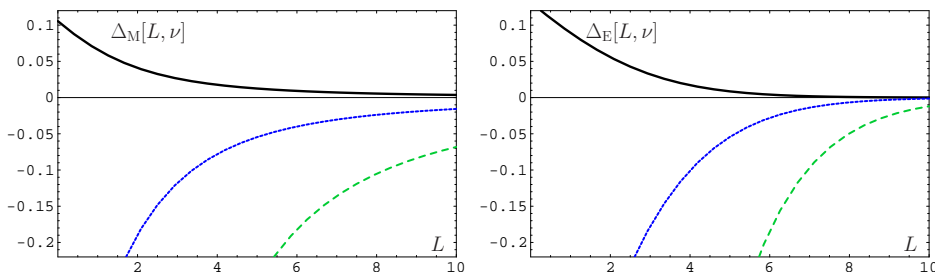


Figure 9: Left panel: Comparing \mathfrak{A}_ν with $(\mathfrak{A}_1)^\nu$ for fractional $\nu = 0.62$ (solid line), 1.62 (dotted line) and 2.62 (dashed line). Right panel: Comparing \mathcal{A}_ν with $(\mathcal{A}_1)^\nu$ for the same fractional values of ν as in the left panel.

The construction of the FAPT with a fixed number of quark flavors, N_f , is a two-step procedure: we start with the perturbative result $[a(Q^2)]^\nu$, generate the spectral density $\bar{\rho}_\nu(\sigma)$ using Eq. (26), and then obtain analytic couplings $\overline{\mathcal{A}}_\nu[L]$ and $\overline{\mathfrak{A}}_\nu[L]$ via Eqs. (27). Here N_f is fixed and factorized out. We can proceed in the same manner for N_f -dependent quantities: $[\alpha_s(Q^2; N_f)]^\nu \Rightarrow \rho_\nu(\sigma; N_f) = \rho_\nu[L_\sigma; N_f] \equiv \bar{\rho}_\nu(\sigma) / b_f^\nu \Rightarrow \mathcal{A}_\nu[L; N_f]$ and $\mathfrak{A}_\nu[L; N_f]$ — here N_f is fixed but not factorized out.

The global version of the FAPT [23], (2009), which takes into account heavy-quark thresholds, is constructed along the same lines but starting from global perturbative coupling $[\alpha_s^{\text{glob}}(Q^2)]^\nu$, being a continuous function of Q^2 due to choosing different values of QCD scales Λ_f , corresponding to different values of N_f . We illustrate here the case of only one heavy-quark threshold at $Q^2 = m_4^2$, corresponding to the transition $N_f = 3 \rightarrow N_f = 4$. Then we obtain the discontinuous spectral density

$$\rho_n^{\text{glob}}(\sigma) = \theta(L_\sigma < L_4) \rho_n[L_\sigma; 3] + \theta(L_4 \leq L_\sigma) \rho_n[L_\sigma + \lambda_4; 4], \quad (30)$$

with $L_\sigma \equiv \ln(\sigma/\Lambda_3^2)$, $L_f \equiv \ln(m_f^2/\Lambda_3^2)$ and $\lambda_f \equiv \ln(\Lambda_3^2/\Lambda_f^2)$ for $f = 4$,

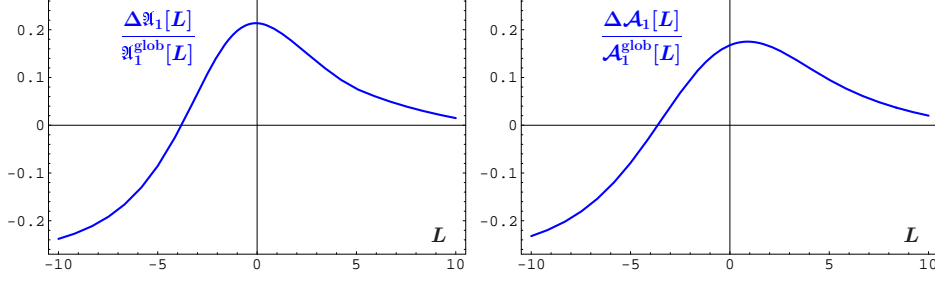


Figure 10: Left: Deviation of the global coupling relative to the fixed- N_f coupling in the FAPT: $\Delta\mathfrak{A}_1[L]/\mathfrak{A}_1^{\text{glob}}[L]$. Right: The same for $\Delta\mathcal{A}_1[L]/\mathcal{A}_1^{\text{glob}}[L]$.

which is expressed in terms of the fixed-flavor spectral densities with 3 and 4 flavors, $\rho_n[L_\sigma; 3]$ and $\rho_n[L_\sigma + \lambda_4; 4]$; note here that $L_\sigma + \lambda_4 = \ln(\sigma/\Lambda_4^2)$. However, it generates the continuous Minkowskian coupling

$$\mathfrak{A}_\nu^{\text{glob}}[L] = \theta(L < L_4) \left(\mathfrak{A}_\nu[L; 3] + \Delta_{43}\mathfrak{A}_\nu \right) + \theta(L_4 \leq L) \mathfrak{A}_\nu[L + \lambda_4; 4] \quad (31a)$$

with $\Delta_{43}\mathfrak{A}_\nu = \mathfrak{A}_\nu[L_4 + \lambda_4; 4] - \mathfrak{A}_\nu[L_4; 3]$ and the analytic Euclidean coupling $\mathcal{A}_\nu^{\text{glob}}[L]$

$$\mathcal{A}_\nu^{\text{glob}}[L] = \mathcal{A}_\nu[L + \lambda_4; 4] + \int_{-\infty}^{L_4} \frac{\bar{\rho}_\nu[L_\sigma; 3] - \bar{\rho}_\nu[L_\sigma + \lambda_4; 4]}{1 + e^{L-L_\sigma}} dL_\sigma. \quad (31b)$$

To demonstrate the magnitude of the threshold corrections, we show in Fig. 10 the values of the normalized deviations $\Delta\mathcal{A}_\nu[L] = \mathcal{A}_\nu^{\text{glob}}[L] - \mathcal{A}_\nu[L + \lambda_4; 4]$ and $\Delta\mathfrak{A}_\nu[L] = \mathfrak{A}_\nu^{\text{glob}}[L] - \mathfrak{A}_\nu[L + \lambda_4; 4]$ in the Euclidean and Minkowski domains, respectively (for more details see [25]).

2.4. Electromagnetic pion form factor at NLO

The scaled hard-scattering amplitude truncated at the next-to-leading order (NLO) and evaluated at renormalization scale $\mu_R^2 = \lambda_R Q^2$ reads (see for details [29])

$$T_{\text{H}}^{\text{NLO}}(x, y, Q^2; \mu_F^2, \lambda_R Q^2) = \alpha_s(\lambda_R Q^2) t_{\text{H}}^{(0)}(x, y) + \frac{\alpha_s^2(\lambda_R Q^2)}{4\pi} \left\{ C_{\text{F}} t_{\text{H},2}^{(1,\text{F})} \left(x, y; \frac{\mu_F^2}{Q^2} \right) + b_0 t_{\text{H}}^{(1,\beta)}(x, y; \lambda_R) + t_{\text{H}}^{(\text{FG})}(x, y) \right\} \quad (32)$$

with shorthand notation ($\bar{x} \equiv 1 - x$)

$$t_{\text{H},2}^{(1,\text{F})} \left(x, y; \frac{\mu_F^2}{Q^2} \right) = t_{\text{H}}^{(0)}(x, y) \left[2 \left(3 + \ln(\bar{x}\bar{y}) \right) \ln \frac{Q^2}{\mu_F^2} \right].$$

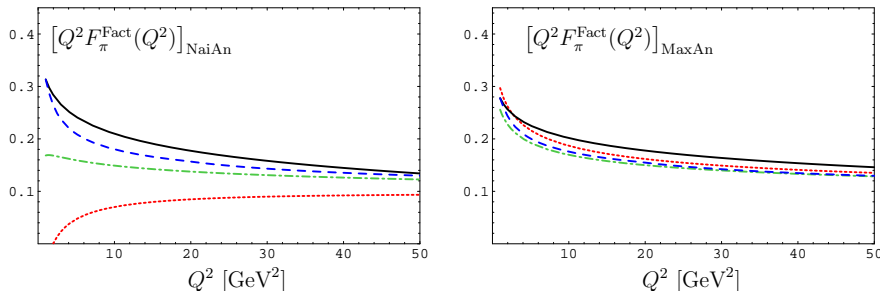


Figure 11: Factorized pion FF in the “Naive Analytization” (left panel) and in the “Maximal Analytization” (right panel). Solid lines correspond to the scale setting $\mu_R^2 = 1 \text{ GeV}^2$, dashed lines — to $\mu_R^2 = Q^2$, dotted lines — to the BLM prescriptions, whereas dash-dotted lines — to the α_v -scheme.

The leading twist-2 pion distribution amplitude (DA) [30] at the normalization scale μ_F^2 is given by [31]

$$\varphi_\pi(x, \mu_F^2) = 6x(1-x) \left[1 + \sum_{n \geq 1} a_{2n}(\mu_F^2) C_{2n}^{3/2}(2x-1) \right].$$

All nonperturbative information is encapsulated in the Gegenbauer coefficients $a_{2n}(\mu_F^2)$. To obtain the factorized part of the pion form factor (FF), one needs to convolute the pion DA with the hard-scattering amplitude:

$$F_\pi^{\text{Fact}}(Q^2) = \varphi_\pi(x; \mu_F^2) \otimes_x T_H^{\text{NLO}}(x, y; \mu_F^2, Q^2) \otimes_y \varphi_\pi(y; \mu_F^2).$$

In order to obtain the analytic expression for the pion FF at the NLO the so-called “Naive Analytization” was suggested in [32]. It uses the analytic image \mathcal{A}_1 only for coupling itself but not for its powers. In contrast and in full accord with the APT ideology the receipt of “Maximal Analytization” has recently been proposed in [29], which uses the analytic image \mathcal{A}_2 for the second power of coupling as well. In Fig. 11 we show the predictions for the factorized pion FF in the “Naive” and the “Maximal Analytization” approaches. We see that in the “Maximal Analytization” approach the obtained results are practically insensitive to the renormalization scheme and scale-setting choice (already at the NLO level). It is interesting to note here that the FAPT approach, used in [23] for analytization of the $\ln(Q^2/\mu_F^2)$ -terms in the hard amplitude (32), diminishes also the dependence on the factorization scale setting in the interval $\mu_F^2 = 1 - 50 \text{ GeV}^2$.

Using the FAPT it appears to be possible to estimate the NNLO correction to the whole pion FF without very complicated calculation of the corresponding three-loop triangle spectral density [33]. Here we show in Fig. 12 only the results: The NNLO correction is of the order of 3 – 10%.

2.5. Resummation in the one-loop APT and FAPT

We consider now the perturbative expansion of a typical physical quantity, like the Adler function and the ratio \bar{R} , in the one-loop APT. Due to limited space of our presentation we provide all formulas only for quantities in the Minkowski region:

$$\mathcal{R}[L] = \sum_{n=1}^{\infty} d_n \bar{\mathfrak{A}}_n[L]. \quad (33)$$

We suggest that there exists a generating function $P(t)$ for the coefficients $\tilde{d}_n = d_n/d_1$:

$$\tilde{d}_n = \int_0^{\infty} P(t) t^{n-1} dt \quad \text{with} \quad \int_0^{\infty} P(t) dt = 1. \quad (34)$$

To shorten our formulae, we use for the integral $\int_0^{\infty} f(t) P(t) dt$ the following notation: $\langle\langle f(t) \rangle\rangle_{P(t)}$. Then the coefficients $d_n = d_1 \langle\langle t^{n-1} \rangle\rangle_{P(t)}$ and, as has been shown in [24], we have the exact result for the sum in (33)

$$\mathcal{R}[L] = d_1 \langle\langle \bar{\mathfrak{A}}_1[L-t] \rangle\rangle_{P(t)}. \quad (35)$$

The integral in variable t here has a rigorous meaning ensured by the finiteness of the coupling $\bar{\mathfrak{A}}_1[t] \leq 1$ and fast fall-off of the generating function $P(t)$.

In our previous publications [25], we constructed generalizations of these results, first, to the case of the global APT when heavy-quark thresholds are taken into account. Then one starts with the series of type (33), where $\bar{\mathfrak{A}}_n[L]$ are substituted by their global analogs $\mathfrak{A}_n^{\text{glob}}[L]$ (note that due to

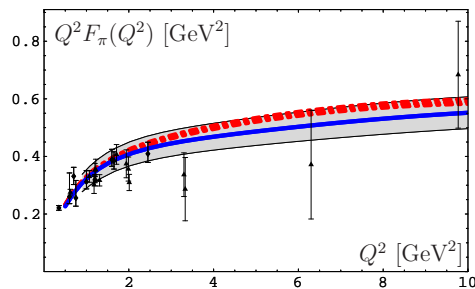


Figure 12: We show as a narrow dashed-dotted strip the predictions for the pion FF obtained using the improved Gaussian model of the nonlocal QCD vacuum. The width of the strip is due to the variation of the Gegenbauer coefficients a_2 and a_4 in the corresponding shaded bands for the pion DA (indicated by the central solid line). Note that this dashed-dotted strip shows the effect of the $O(\mathcal{A}_2)$ correction only for the central solid curve of the shaded band.

different normalizations of global couplings, $\mathfrak{A}_n^{\text{glob}}[L] \simeq \bar{\mathfrak{A}}_n[L]/\beta_f^n$, the coefficients d_n should also be changed). Then

$$\begin{aligned} \mathcal{R}^{\text{glob}}[L] &= d_1 \theta(L < L_4) \langle \langle \Delta_4 \mathfrak{A}_1[t] + \mathfrak{A}_1\left[L - \frac{t}{\beta_3}; 3\right] \rangle \rangle_{P(t)} \\ &+ d_1 \theta(L \geq L_4) \langle \langle \mathfrak{A}_1\left[L + \lambda_4 - \frac{t}{\beta_4}; 4\right] \rangle \rangle_{P(t)}; \end{aligned} \quad (36)$$

where $\Delta_4 \mathfrak{A}_\nu[t] \equiv \mathfrak{A}_\nu\left[L_4 + \lambda_4 - t/\beta_4; 4\right] - \mathfrak{A}_\nu\left[L_3 - t/\beta_3; 3\right]$.

The second generalization has been obtained for the global FAPT. Then the starting point is the series of the type $\sum_{n=0}^{\infty} d_n \mathfrak{A}_{n+\nu}^{\text{glob}}[L]$ and the result of summation is a complete analog of Eq. (36) with the substitutions

$$P(t) \Rightarrow P_\nu(t) = \int_0^1 P\left(\frac{t}{1-x}\right) \frac{\nu x^{\nu-1} dx}{1-x}, \quad (37)$$

$d_0 \Rightarrow d_0 \mathfrak{A}_\nu[L]$, $\mathfrak{A}_1[L-t] \Rightarrow \mathfrak{A}_{1+\nu}[L-t]$, and $\Delta_4 \mathfrak{A}_1[t] \Rightarrow \Delta_4 \mathfrak{A}_{1+\nu}[t]$. All needed formulas have also been obtained in parallel for the Euclidean case, for details see [25].

2.6. Applications to Higgs boson decay

Here we analyze the Higgs boson decay to a $\bar{b}b$ pair. For its width we have

$$\Gamma(\text{H} \rightarrow \bar{b}b) = \frac{G_F}{4\sqrt{2}\pi} M_H \tilde{R}_s(M_H^2) \quad (38)$$

with $\tilde{R}_s(M_H^2) \equiv m_b^2(M_H^2) R_s(M_H^2)$ and $R_s(s)$ is the R -ratio for the scalar correlator, for details see [23, 34]. In the one-loop FAPT this generates the following non power expansion¹¹:

$$\tilde{R}_s[L] = 3 \hat{m}_{(1)}^2 \left\{ \mathfrak{A}_{\nu_0}^{\text{glob}}[L] + d_1^S \sum_{n \geq 1} \frac{\tilde{d}_n^S}{\pi^n} \mathfrak{A}_{n+\nu_0}^{\text{glob}}[L] \right\}, \quad (39)$$

where $\hat{m}_{(1)}^2 = 9.05 \pm 0.09 \text{ GeV}^2$ is the RG-invariant of the one-loop $m_b^2(\mu^2)$ evolution $m_b^2(Q^2) = \hat{m}_{(1)}^2 \alpha_s^{\nu_0}(Q^2)$ with $\nu_0 = 2\gamma_0/b_0(5) = 1.04$ and γ_0 is the quark-mass anomalous dimension. This value $\hat{m}_{(1)}^2$ was obtained using the one-loop relation [35] between the pole b -quark mass of [36] and the mass $m_b(m_b)$.

¹¹Appearance of denominators π^n in association with the coefficients \tilde{d}_n is due to d_n normalization.

We take for the generating function $P(t)$ the Lipatov-like model of [25] with $\{c = 2.4, \beta = -0.52\}$

$$\tilde{d}_n^S = c^{n-1} \frac{\Gamma(n+1) + \beta \Gamma(n)}{1 + \beta} \quad \text{with} \quad P_S(t) = \frac{(t/c) + \beta}{c(1 + \beta)} e^{-t/c}. \quad (40)$$

It gives a very good prediction for \tilde{d}_n^S with $n = 2, 3, 4$, calculated in the QCD PT [34]: 7.50, 61.1, and 625 in comparison with 7.42, 62.3, and 620. It is worthwhile to remind here the history of calculating the β -function coefficients β_n in the φ_4^4 scalar field theory. In [37] the resummation procedure was suggested on the basis of taking into account four-loop results in the MOM scheme. The five-loop calculations of the anomalous dimensions γ_2 and γ_4 for this model in the $\overline{\text{MS}}$ scheme was performed in [38] (γ_2) and in [39] (γ_4 was calculated numerically with small errors). In this last paper, using the Borel-like technique and the four-loop results in the $\overline{\text{MS}}$ scheme the five-loop prediction $\beta_5^{\text{resum}} = 1405 \pm 80$ was made. The calculated result $\beta_5 = 1420.69$ appeared in the range predicted in [37]. The uncertainties of numerical calculations were eliminated by Kazakov [40] using the uniqueness method for multiloop calculations — he confirmed numerical results. After that, in [41], the errors in the previous results for both γ_2 and γ_4 were revealed. As a result, γ_2 and γ_4 were changed, but the value of β_5 numerically appears to be practically the same! Resume: resummation predictions for the $\overline{\text{MS}}$ -scheme β_5 are really in very good accord with the five-loop results.

Then we apply the FAPT resummation technique to estimate how good is it in approximating the whole sum $\tilde{\mathcal{R}}_S[L]$ in the range $L \in [11.5, 13.7]$ which corresponds to $M_H \in [60, 180]$ GeV² with $\Lambda_{\text{QCD}}^{N_f=3} = 189$ MeV and $\mathfrak{A}_1^{\text{glob}}(m_Z^2) = 0.122$. In this range, we have

$$\frac{\tilde{\mathcal{R}}_S[L]}{3\hat{m}_{(1)}^2} = \mathfrak{A}_{\nu_0}^{\text{glob}}[L] + \frac{d_1^S}{\pi} \langle \langle \mathfrak{A}_{1+\nu_0} \left[L + \lambda_5 - \frac{t}{\pi\beta_5}; 5 \right] \Delta_6 \bar{\mathfrak{A}}_{1+\nu_0} \left[\frac{t}{\pi} \right] \rangle \rangle_{P_{\nu_0}^S} \quad (41)$$

with $L_6 = \ln(m_t^2/\Lambda_3^2)$ and $P_{\nu_0}^S(t)$ defined via Eqs. (40) and (37). Now we analyze the accuracy of the truncated FAPT expressions

$$\tilde{\mathcal{R}}_S[L; N] = 3\hat{m}_{(1)}^2 \left[\mathfrak{A}_{\nu_0}^{\text{glob}}[L] + d_1^S \sum_{n=1}^N \frac{\tilde{d}_n^S}{\pi^n} \mathfrak{A}_{n+\nu_0}^{\text{glob}}[L] \right] \quad (42)$$

and compare them with the total sum $\tilde{\mathcal{R}}_S[L]$ in Eq. (41) using relative errors $\Delta_N[L] = 1 - \tilde{\mathcal{R}}_S[L; N]/\tilde{\mathcal{R}}_S[L]$. In Fig. 13, we show these errors for $N = 2$, $N = 3$, and $N = 4$ in the analyzed range of $L \in [11, 13.8]$. We see that already $\tilde{\mathcal{R}}_S[L; 2]$ gives accuracy of the order of 2.5%, whereas $\tilde{\mathcal{R}}_S[L; 3]$ of the order of 1%. Looking at Fig. 13 we understand that only in order to have the accuracy better than 0.5%, one needs to take into account the 4-th

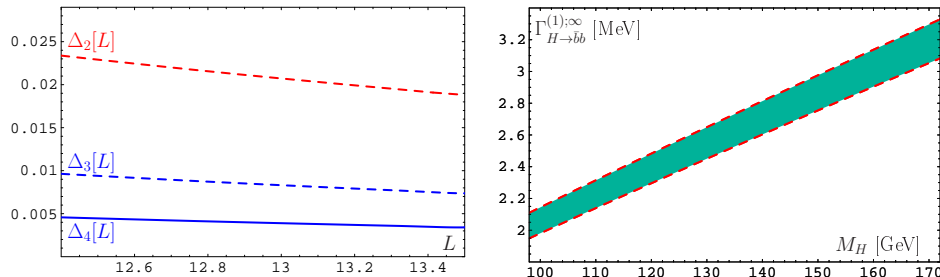


Figure 13: Left panel: The relative errors $\Delta_N[L]$, $N = 2, 3$ and 4 , of the truncated FAPT in comparison with the exact summation result, Eq. (41). Right panel: The width $\Gamma_{H \rightarrow b\bar{b}}^{(1)\infty}$ as a function of the Higgs boson mass M_H in the resummed FAPT. The width of the shaded strip is due to the overall uncertainties induced by the uncertainties of the resummation procedure and the pole mass error-bars. Both panels show the results obtained in the one-loop FAPT [25].

correction. We verified also that the uncertainty due to $P(t)$ -modelling is small $\lesssim 0.6\%$, while the on-shell mass uncertainty is of the order of 2% . The overall uncertainty then is of the order of 3% , see in the right panel of Fig. 13, that is in agreement with the Kataev&Kim estimations [35].

3. Conclusions

- Perturbation approach in Quantum theory (both the nonrelativistic and QFT) suffers from divergence of (asymptotic) series in powers of small expansion parameter g . The reason is the nonanalyticity (essential singularity) at the origin of the g complex plane. Due to this, common power expansions have a lower limit of accuracy (as shown in Table 1). In particular, this refers to perturbative QCD. There, for some low-energy processes (see Table 2) this lower limit exceeds the experimental error. This is the reason that the nonperturbative means are of utmost importance in many physical situations.
- In Section 1, two of the nonperturbative instruments, the *Renormalization Group* and the *Dispersion Relation* methods, are outlined; description of their application to the actual case of Quantum Chromodynamics then follows. Here, the particular theoretical construction, the Analytic Perturbation Theory (APT), was devised on the turn of the century.
- Section 2 begins with the summary of the APT basic elements. We also remind that in the APT one has
 - Universal (loop & scheme independent) IR limit;
 - Practical renormalization-scheme independence;
 - Non-power perturbation expansion over a set of particular functions $\mathcal{A}_n(Q^2)$, $\mathfrak{A}_n(s)$ instead of the running coupling powers $\alpha_s(\dots)^n$;
 - Quick loop convergence that improves the situation with the role of higher-loop corrections.

- As a result of quick loop convergence, we show (see Table 3) that 3- and 4-loop APT terms contribute to observables less than 5%, i.e., below the current level of data errors. Hence, the two-loop, NNLO level is practically sufficient.
- Then we expose the Fractional APT (FAPT) that provides an effective tool to apply the APT approach for renormgroup-improved perturbative amplitudes. By the example of the pion electromagnetic form factor we show that the FAPT delivers minimal sensitivity to both renormalization and factorization scale setting.
- In both the APT and FAPT approaches we describe the resummation procedures that produce finite resummed answers for perturbative quantities if one knows the generating functions $P(t)$ for the PT coefficients. Using quite simple model generating function $P_S(t)$ for Higgs boson decay $H \rightarrow \bar{b}b$ we conclude that at N³LO we have accuracy of the order of 1% due to the truncation error and of the order of 2% due to the RG-invariant mass uncertainty.

Acknowledgements

It is a pleasure to thank Drs. Sergey Mikhailov and Oleg Teryaev for numerous discussions and useful remarks. The fruitful remarks and discussions with Drs. Konstantin Chetyrkin, Andrey Grozin, Andrey Kataev, Alexey Pivovarov, Anatoly Radyushkin, and Nico Stefanis are also greatly acknowledged by one of the authors (A. B.).

References

- [1] F. J. Dyson, *Phys. Rev.* **85** (1952) 631.
- [2] D. I. Kazakov and D. V. Shirkov, *Fortsch. Phys.* **28** (1980) 465.
- [3] L. N. Lipatov, *Sov. Phys. JETP* **45** (1977) 216.
- [4] Charles Angas Hurst, *Proc. Cambridge Phil. Soc.* **48** (1952) 625; Walter E. Thirring, *Helv. Phys. Acta* **26** (1953) 33; A. Petermann, *Phys. Rev.* **89** (1953) 1160.
- [5] D. V. Shirkov, *Nuovo Cim. Lett.* **18** (1977) 452; B. D. Dorfel, D. I. Kazakov, and D. V. Shirkov, JINR Preprint E2-10720 (1977).
- [6] H. F. Jones and I. L. Solovtsov, *Phys. Lett.* B349 (1995) 519 [hep-ph/9501344]; D. V. Shirkov and I. L. Solovtsov, *JINR Rapid Comm.* 2[76] (1996) 5 [hep-ph/9604363]; *Phys. Rev. Lett.* **79** (1997) 1209 [hep-ph/9704333]; K. A. Milton and I. L. Solovtsov, *Phys. Rev. D* **55** (1997) 5295 [hep-ph/9611438].
- [7] D. V. Shirkov, “Evolution of the Bogoliubov Renormalization Group”, in *Quantum Field Theory, A XXth century profile*, Ed. Asoke N. Mitra, Hindustan Book Agency, INSA, New Dehli, 2000, pp. 26–58 [hep-th/9909024]; V. F. Kovalev and D. V. Shirkov, *Phys. Repts.* **352** (2001) 219–249 [hep-th/0001210].
- [8] G. S. Golitsyn, “The portrait of an unknown person”, *Priroda* **6** (2007) 61 (in Russian).
- [9] N. N. Bogoliubov and D. V. Shirkov, *Nuovo Cim.* **3** (1956) 845.
- [10] N. N. Bogoliubov and D. V. Shirkov, *Introduction to the Theory of Quantum Fields* Wiley, New York, 1980, 720 p.

-
- [11] P. A. M. Dirac, in *Septième Conseil du Physique Solway, Bruxelles, October 22–29, 1933*, Ed. J. Cockcroft *et al.* (Gauthier-Villars, Paris, 1934), p. 203.
- [12] D. V. Shirkov, *Nucl.Phys.* **B371** (1992) 467–481.
- [13] G. Källén, *Helv. Phys. Acta* **25** (1952) 417.
- [14] N. N. Bogoliubov, A. A. Logunov, and D. V. Shirkov, *Sov. Phys. JETP* **10** (1960) 574.
- [15] S. Bethke, *Prog. Part. Nucl. Phys.* **58** (2007) 351 [HEP-EX/0606035].
- [16] R. S. Pasechnik *et al.*, *Phys. Rev.* **D78** (2008) 071902 [ArXiv:0808.0066 [hep-ph]]; *Phys. Rev.* **D81** (2010) 016010 [ArXiv:0911.3297 [hep-ph]]; V. L. Khandramai *et al.*, paper in preparation.
- [17] D. V. Shirkov and I. L. Solovtsov, *Theor. Math. Phys.* **150** (2007) 132 [hep-ph/0611229].
- [18] D. V. Shirkov, *Theor. Math. Phys.* **132** (2002) 1307–1317 [hep-ph/0208082]; G. M. Prospero, M. Raciti, and C. Simolo, *Prog. Part. Nucl. Phys.* **58** (2007) 387 [hep-ph/0607209].
- [19] A. V. Radyushkin, *JINR Rapid Commun.* **78** (1996) 96 [JINR Preprint, E2-82-159, hep-ph/9907228]; N. V. Krasnikov and A. A. Pivovarov, *Phys. Lett.* **B116** (1982) 168.
- [20] K. A. Milton, I. L. Solovtsov, and O. P. Solovtsova, *Phys. Lett.* **B415** (1997) 104 [hep-ph/9706409]; Kimball A. Milton and Olga P. Solovtsova, *Phys. Rev.* **D57** (1998) 5402 [hep-ph/9710316]; I. L. Solovtsov and D. V. Shirkov, *Phys. Lett.* **B442** (1998) 344 [hep-ph/9711251]; A. P. Bakulev, A. V. Radyushkin, and N. G. Stefanis, *Phys. Rev.* **D62** (2000) 113001 [hep-ph/0005085]; D. V. Shirkov, *Theor. Math. Phys.* **127** (2001) 409 [hep-ph/0012283]; *Eur. Phys. J.* **C22** (2001) 331 [hep-ph/0107282].
- [21] D. V. Shirkov, *Lett. Math. Phys.* **48** (1999) 135.
- [22] Y. A. Simonov, *Phys. Atom. Nucl.* **65** (2002) 135 [hep-ph/0109081]; ArXiv:1011.5386 [hep-ph].
- [23] A. P. Bakulev, S. V. Mikhailov, and N. G. Stefanis, *Phys. Rev.* **D72** (2005) 074014, 119908(E) [hep-ph/0506311]; *Phys. Rev.* **D75** (2007) 056005; **D77** (2008) 079901(E) [hep-ph/0607040]; A. P. Bakulev, A. I. Karanikas, and N. G. Stefanis, *Phys. Rev.* **D72** (2005) 074015 [hep-ph/0504275]; A. P. Bakulev, *Phys. Part. Nucl.* **40** (2009) 715 [arXiv:0805.0829 [hep-ph]]; N. G. Stefanis, ArXiv:0902.4805 [hep-ph].
- [24] S. V. Mikhailov, *JHEP* **0706** (2007) 009 [hep-ph/0411397].
- [25] A. P. Bakulev and S. V. Mikhailov, in *Proceedings of International Seminar on Contemporary Problems of Elementary Particle Physics, Dedicated to the Memory of I. L. Solovtsov, Dubna, January 17–18, 2008.*, Eds. A. P. Bakulev *et al.* (JINR, Dubna, 2008), pp. 119–133 [ArXiv:0803.3013 [hep-ph]]; A. P. Bakulev, S. V. Mikhailov, and N. G. Stefanis, *JHEP* **1006** (2010) 085 [ArXiv:1004.4125 [hep-ph]].
- [26] M. Baldicchi *et al.*, *Phys. Rev. Lett.* **99** (2007) 242001 [ArXiv:0705.0329 [hep-ph]]; *Phys. Rev.* **D77** (2008) 034013 [ArXiv:0705.1695 [hep-ph]].
- [27] B. A. Magradze, *Few Body Syst.* **48** (2010) 143 [ArXiv:1005.2674 [hep-ph]].
- [28] A. I. Karanikas and N. G. Stefanis, *Phys. Lett.* **B504** (2001) 225; *ibid.* **B636** (2006) 330–331(E) [hep-ph/0101031].
- [29] A. P. Bakulev *et al.*, *Phys. Rev.* **D70** (2004) 033014 [hep-ph/0405062].
- [30] A. V. Radyushkin, Dubna preprint P2-10717, 1977 [hep-ph/0410276].
- [31] A. V. Efremov and A. V. Radyushkin, *Phys. Lett.* **B94** (1980) 245.
- [32] N. G. Stefanis, W. Schroers, and H.-C. Kim, *Phys. Lett.* **B449** (1999) 299; *Eur. Phys. J.* **C18** (2000) 137 [hep-ph/0005218].

-
- [33] A. P. Bakulev, A. V. Pimikov, and N. G. Stefanis, *Phys. Rev.* **D79** (2009) 093010 [ArXiv:0904.2304 [hep-ph]].
 - [34] P. A. Baikov, K. G. Chetyrkin, and J. H. Kühn, *Phys. Rev. Lett.* **96** (2006) 012003 [hep-ph/0511063].
 - [35] A. L. Kataev and V. T. Kim, in *Proceedings of International Seminar on Contemporary Problems of Elementary Particle Physics, Dedicated to the Memory of I. L. Solovtsov, Dubna, January 17–18, 2008.*, Eds. A. P. Bakulev *et al.* (JINR, Dubna, 2008), pp. 167–182 [ArXiv:0804.3992 [hep-ph]]; *PoS ACAT08* (2009) 004.
 - [36] Johann H. Kühn and M. Steinhauser, *Nucl. Phys.* **B619** (2001) 588 [hep-ph/0109084].
 - [37] D. I. Kazakov, D. V. Shirkov, and O. V. Tarasov, *Theor. Math. Phys.* **38** (1979) 9.
 - [38] K. G. Chetyrkin, A. L. Kataev, and F. V. Tkachov, *Phys. Lett.* **B99** (1981) 147.
 - [39] S. G. Gorishnii *et al.*, *Phys. Lett.* **B132** (1983) 351.
 - [40] D. I. Kazakov, *Phys. Lett.* **B133** (1983) 406.
 - [41] H. Kleinert *et al.*, *Phys. Lett.* **B272** (1991) 39 [hep-th/9503230].